Determination of the effective thermal conductivity of granular materials under varying pressure conditions

E. S. Huetter,[1] N. I. Koemle,[1] G. Kargl,[1] and E. Kaufmann[1]

Received 22 January 2008; revised 17 July 2008; accepted 3 September 2008; published 4 December 2008.

[1] We report on thermal conductivity measurements performed on glass spheres of different grain sizes under varying pressure conditions ranging from 10^{-5} up to 1000 hPa. Glass spheres of 0.1 up to 4.3 mm were used as an analogue for the coarse-grained fractions of planetary regolith. From the obtained conductivity versus pressure data, sample pore sizes were derived and compared to estimated pore sizes. An increasing difference between derived and estimated pore size with increasing grain size was found. The behavior of the granular matter with decreasing pressure was analyzed by estimating the Knudsen number for the given system. The results indicate a high variability of the effective thermal conductivity for Martian conditions. Furthermore, the results imply that the thermal conductivity reaches a grain size-dependent, but pressure-independent, value for pressures below 0.01 hPa. For vacuum conditions a linear relation between grain size and effective thermal conductivity was found. Additionally, a mixture was analyzed, which showed a stronger decrease with gas pressure compared to the single-sized samples. From the pore size derived for the mixture an "effective" grain size composed of weighted mean of the mixture components was determined.

Citation: Huetter, E. S., N. I. Koemle, G. Kargl, and E. Kaufmann (2008), Determination of the effective thermal conductivity of granular materials under varying pressure conditions, *J. Geophys. Res.*, *113*, E12004, doi:10.1029/2008JE003085.

1. Introduction

[2] Many planetary bodies of our solar system, notably bodies not protected by atmospheres, like the Moon, Mars, and Mercury, but also the satellites of the outer solar system, comets and asteroids are covered by so-called regolith layers. This material occupies the surface layers of these bodies and has a texture ranging from micrometer-sized particles up to boulders with sizes in the meter range [*Vaniman et al.*, 1991]. Regolith mainly consists of the planetary body's bedrock material, processed by impact meteorite gardening. The bulk of regolith was produced during the period of late heavy bombardment which occurred approximately 3.8–4.1 Ga ago. Later on up to the present time the continuous flux of micrometeorites toward these surfaces led to further reduction of typical grain sizes in the near-surface layers of the regolith. These layers form the boundary between the interior of the body and its outer environment. Thus, their thermophysical properties, especially the effective thermal conductivity, control to a high extent the energy balance of these bodies as a whole. Unfortunately, until now in situ measurements of the thermal conductivity have only been carried out on the Moon in the frame of the Apollo 15 and the Apollo 17 mission. Thermal conductivity values of 0.015 up to 0.03 W m^{-1} K^{-1} were found in a depth of 1 to 2.36 m. Currently, after a period of lesser interest, the Moon is again a topic of active research. Several missions from various countries including rovers for in situ measurements are planned. Along with cameras and spectrometers to determine the surface chemical composition, thermal experiments are included in the planned payload. Furthermore, first in situ thermal conductivity values have recently been obtained at Mars by the Phoenix Mars Lander. In section 2 we give a short overview of the theory of heat transfer in particulate media and prior laboratory measurements of this phenomenon. Subsequently, the material and the applied measurement method are described in sections 3 and 4, followed by a description of the measurement procedure and the measurement setup in section 5. The measurement results are presented in section 6.

2. Heat Transfer in Granular Media

[3] The conduction of heat through a porous medium depends on the texture of the material and the thermal conductivities of the participating phases [*Kaviany*, 1998]. The spatial distribution of the solid and the fluid phase can be described by the porosity ψ, which is defined as the ratio of the volume filled by the fluid to the total volume. Alternatively, the porosity can also be expressed by the ratio of the density difference between particle material density and bulk density to particle material density:

$$\psi = \frac{V_f}{V_{tot}} = 1 - \frac{\rho_{bulk}}{\rho_{solid}} \quad (1)$$

[1]Space Research Institute, Austrian Academy of Sciences, Graz, Austria.

0148-0227/08/2008JE003085

Additionally, the other modes of heat transfer, namely radiation and convection, may contribute. Thus, in general, the overall effective thermal conductivity of a granular medium can be given as the sum of the "conductivities" related to different heat transfer processes. As a matter of fact, the majority of the various models and relations for the effective thermal conductivity of granular material that can be found in literature take into account the influences of the conductivities of the participating phases and their spatial distribution. The radiative and convective contributions are modeled separately. Commonly used models for determining the effective thermal conductivity of granular materials are, e.g., given by *Chauk and Fan* [1998] or *Woodside and Messmer* [1961]. In a dry system of solid particles and gas the gaseous phase controls the overall effective thermal conductivity. This is because the bigger part of the particle surface is in contact with the gas molecules in the pores and only small areas are in contact with other particles. Furthermore, the heat transfer via the contact areas is hindered by the surface roughness of the particles. So the major part of the heat transfer takes place via gas molecule interaction and gas molecule/particle surface interaction. A dimensionless parameter, characterizing the gas behavior in a porous medium is the Knudsen number, which is given as the ratio between the mean free path of the gas molecules and the average pore size:

$$\mathrm{Kn} = \frac{\text{mean free path of the gas molecules}}{\text{average pore size}} = \frac{\lambda}{\delta_p} = \frac{k_b T}{\sqrt{2}\pi d_g^2 p \delta_p} \quad (2)$$

For Knudsen numbers Kn > 10 [*Kaviany*, 1998] molecule pore wall collisions are dominating. That implies that hardly any intergaseous conduction takes place. Therefore, in the absence of phase transitions, where large amounts of energy could be transported from pore wall to pore wall by the remaining gas molecules, the gaseous contribution is negligible. The average pore size (also referred to as interparticle distance) depends on the configuration and size of the particles. For the case of spherical particles in random arrangement the pore size can be estimated by using [*Kaviany*, 1994]:

$$\delta_p = \left[\frac{0.905}{(1-\psi)^{\frac{1}{3}}} - 1\right] d_p \quad (3)$$

In vacuum the effective thermal conductivity is finally reduced to contributions from heat transfer via the solid phase (contact points of the particles) and radiation [*Huetter and Koemle*, 2008]. In this case the effective thermal conductivity can be expressed as

$$k_{vac} = k_{solid} + k_{rad} \quad (4)$$

The contribution due to radiation k_{rad} was found to be proportional to T^3 [*Howell and Mengüc*, 1998]. The fraction of the vacuum conductivity k_{vac} due to the solid phase k_{solid} includes the influence of porosity and reduced contact area between the particles. For this scenario the radiative and surface properties of the particles have a high influence on the effective thermal conductivity. Moreover, for very small grained particles under ultrahigh vacuum, like on the surface the Moon (10^{-11} hPa), the vacuum conductivity is influenced by adhesive forces between the grains [*Starukhina*, 2000]. A model for the radiative conductivity in a granular medium consisting of spherical particles was proposed by *Schotte* [1960]. He arrived at

$$k_{rad} = \frac{1-\psi}{\frac{1}{k_s} + \frac{1}{4d\sigma\varepsilon\psi T^3}} + 4d\sigma\varepsilon\psi T^3 \quad (5)$$

The effective thermal conductivity of sands under various conditions was investigated by *Woodside and Messmer* [1961]. They suggested a relation for the gaseous conductivity as a function of gas pressure using an effective mean free path λ_{eff}. This effective mean free path can be applied to the kinetic theory relation for the thermal conductivity of a gas. Thereby, equation (7) can be found:

$$\lambda_{eff} = \frac{\lambda \delta_p}{\lambda + \delta_p} \quad (6)$$

$$k_g = \frac{k_g^0 p \delta_p}{p\delta_p + B} \quad (7)$$

The decrease of the effective thermal conductivity due to a decrease of the gaseous conductivity can be approximated by a linear relation (equation (8)). Deviations from this linear correlation appear at the start and at the end of the decrease. Substituting k_g with relation (7) results in a linear relation between the reciprocal conductivity change and reciprocal pressure, given by equation (9). *Woodside and Messmer* [1961] proposed that this correlation could be used to determine the pore size δ_p of a granular material from thermal conductivity versus pressure measurements:

$$k_{eff} = W k_g + k_{vac} \quad (8)$$

$$\frac{1}{k_{eff} - k_{vac}} = \frac{1}{W k_g^0} + \frac{B}{W k_g^0 \delta_p} \frac{1}{p} \quad (9)$$

Further investigations on the thermal conductivity as a function of pressure were done by *Presley and Christensen* [1997a]. They found a linear relationship between effective thermal conductivity and grain size for low pressures and particle sizes smaller than 1 mm. Their investigations [*Presley and Christensen*, 1997a, 1997b] aim at the determination of the effective thermal conductivity of the regolith material occupying the Martian surface. Thermal conductivity studies considering lunar regolith analogs under simulated lunar conditions have been done by *Wechsler and Glaser* [1965]. Investigations of the thermal conductivity of granular materials under vacuum conditions have been conducted, e.g., by *Merrill* [1969], *Watson* [1964], and *Reichenauer et al.* [2007]. However, they did not investigate the influence of grain size on the thermal conductivity.

3. Material

[4] In this work glass beads of five different grain size fractions, ranging from 0.1 up to 4.3 mm (see Figure 1),

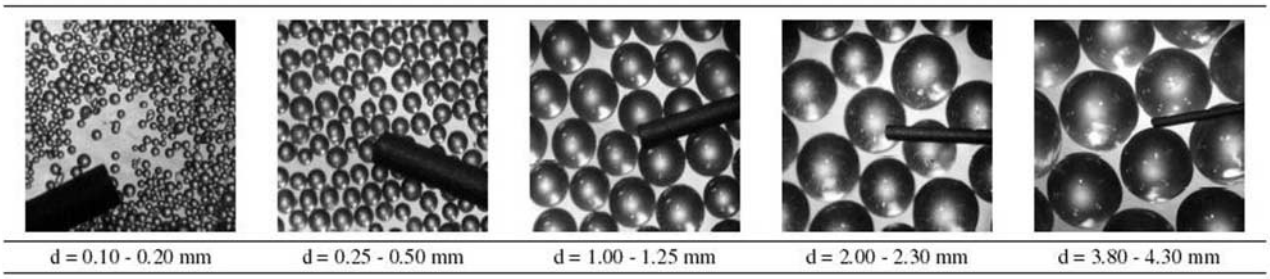

Figure 1. Glass spheres photographed through a microscope. A lead with a diameter of 0.6 mm is displayed for comparison.

were used as a first-order approximation for coarse regolith. The chosen grain sizes complement and extend previous studies [*Presley and Christensen*, 1997a; *Merrill*, 1969; *Watson*, 1964; *Wechsler and Glaser*, 1965] where mostly grain sizes smaller than 1 mm were used. Furthermore, the spherical geometry of the particles is helping comparing the measurement results with results obtained from theoretical models, since many of them presume a spherical geometry of the particles (see section 2). An additional advantage is that the investigated glass beads are all made of the same material. This allows a good recognizability of grain size effects. The chemical composition and physical properties of the glass beads are given in Tables 1a and 1b. The uniformity of the five different size fractions was checked under a microscope for random samples. For all size fractions the effective thermal conductivity was first determined under atmospheric conditions and then at different gas pressures. Supplementary, the effective thermal conductivity of a defined mixture of glass beads, consisting of the three biggest grain sizes (1.00–1.25, 2.00–2.30, and 3.80–4.30 mm), was investigated under varying pressures. Therefore, equal volumes of each of the three grain sizes were mixed. For this case one container was used to scoop equal volumes of each of the three types of glass spheres into the sample container. For every scoop the "scoop container" was carefully filled up to edge. The different size fractions were added in an alternating order. In all from each grain size the same amount of scoop containers was added. Subsequently, the sample was mixed manually by thorough vertical and horizontal stirring. The porosity of all samples was determined by weighing a known volume of the sample and applying equation (1). This was done five times per grain size fraction (each time the volume was refilled) and then the mean value of the five measurement results was calculated. The procedure was repeated for all grain size fractions. The obtained porosities for the different grain sizes ranged between 0.37 and 0.39. The error of these values is ±0.01. This is in good agreement with the porosity values for well-shaken spherical packing's given in literature [e.g., *Kaviany*, 1998]. For the mixture of glass spheres a porosity of 0.355 ± 0.003 was determined in this way.

Table 1a. Chemical Composition of the Used Glass Spheres as Given by the Producer Sigmund Lindner

Element	Fraction (%)
SiO_2	70
Na_2O	13.1
CaO	8.72
MgO	4.1
B_2O_3	2.65
Al_2O_3	0.67
K_2O	0.27
SO_3	0.21
Fe_2O_3	0.09
TiO_2	0.03
BaO, ZnO, Sb_2O_3, As_2O_3, PbO	<0.01

4. Measurement Method

4.1. Measurement Probe

[5] For measuring the effective thermal conductivity, a commercial probe (TP02 thermal conductivity probe) from the Dutch company Hukseflux was used. The design of this sensor is based on the principle of the hot wire method, a well known non steady state technique. The TP02 probe, shown in Figure 2, consists of a heating wire and two thermocouples embedded in a stainless steel tube. One thermocouple is located at the center of the heating wire and reacts to the applied heating, the other is placed at the tip and acts as the reference. This configuration allows the verification that the heat flow only occurs in radial direction (in this case the readings of the thermocouple located at the tip do not change during measurement). Additionally, a temperature-dependent resistor is placed at the base of the instrument. The probe method has already been used very effectively to measure the thermal conductivity of granular materials such as sand, soil and glass spheres [*Wechsler*, 1992; *Koemle et al.*, 2007].

4.2. Data Evaluation

[6] The data evaluation for probe measurements is based on the theory of an infinitely long and thin line heat source embedded in an infinitely extended medium. The medium is heated by the line source with a constant power supply. A solution of the heat conduction equation for this configuration was given by *Carslaw and Jaeger* [1959]. For sufficiently long heating times an approximation for the temperature distribution in response to constant heating can be derived

Table 1b. Physical Properties of the Glass Spheres Used as Sample Material

Properties	Values
k	0.8 W m^{-1} K^{-1}
ρ	2500 kg m^{-3}
ϵ	0.92

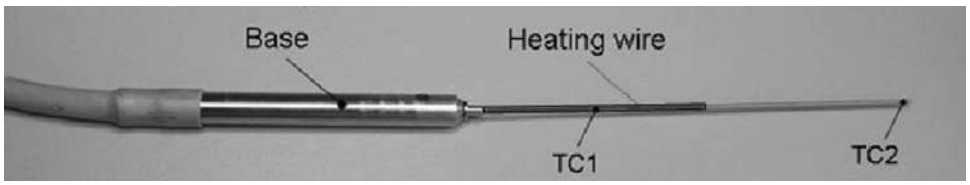

Figure 2. Hukseflux TP02 thermal conductivity measurement probe. The locations of the two thermocouples (TC1 and TC2) and the heating wire are indicated.

by a series expansion. The approximation found in this way leads to a linear relation between the temperature rise and the natural logarithm of time when choosing two points on the time axis (with $t_1 < t_2$) in sufficient distance from the onset of heating:

$$\triangle T = \frac{P_{heat}}{4\pi k} \ln\left(\frac{t_2}{t_1}\right) \tag{10}$$

The slope of the temperature rise with the natural logarithm of time only depends on the applied heating power and the thermal conductivity of the surrounding medium. For a known heating power the latter can be calculated easily from a temperature versus time measurement by linear regression. The linear part was determined by sequential linear fitting of the temperature versus ln(t) data in between the time limits outlined in section 4.3. Sequential fitting means, that a linear fit is applied to a part of the measurement curve (e.g., from 70 to 90 s) and the results are stored. In the next step the data are fitted in between 80 and 100 s, and again the results are stored. This is repeated until the fit interval oversteps the end of the measurement. From the stored regressions the one least deviating from the measurement data is used to determine the thermal conductivity. A typical measurement curve is shown in Figure 3. For the evaluation of the thermal conductivity the part indicated in red was used.

4.3. Boundary Effects

[7] Equation (10) is an approximation only valid for the temperature development after the initial transient period, which can easily be identified in Figure 3. It is reasonable to estimate the duration of the transient time period, if relation (10) is ought to be used. This was done using equation (11) which was derived by *Vos* [1955] and has been successfully applied to measurements performed with the same type of measurement probe as used in this work by *Goodhew and Griffiths* [2004]. A second important fact is that the samples have finite dimensions and boundary effects may occur. This was checked using equation (12), also derived by *Vos* [1955] and applied by *Goodhew and Griffiths* [2004]:

$$t_{trans} > \frac{50 r_{sensor}^2}{4\alpha_{sample}} \tag{11}$$

$$t_{max} = \frac{0.6 R_{sample}^2}{4\alpha_{sample}} \tag{12}$$

For the estimation of t_{trans} and $t_{\max}$ tabulated thermal diffusivity values for dry and water saturated glass beads (16×10^{-8} and 28×10^{-8} $m^2 s^{-1}$) were used. It was found that for the used probe and sample dimensions, the transient period should last for at least 44 s for the dry and 25 s for the water saturated glass beads. Boundary effects may occur after about 17 h in the saturated glass spheres and after approximately one day in the dry glass beads. These results indicate, that for the typical measurement times between 100 and 200 s boundary effects do not play a role, but nevertheless the time interval for the calculation of the thermal conductivity has to be chosen carefully. The operational reliability of the measurement probe was assured by calibrating the sensor in Agar and in Teflon. The derived thermal conductivities for these well known materials were within a range of ±3% of the tabulated values.

5. Experimental Setup and Measurement Description

[8] The thermal conductivity of the glass beads was investigated in a pressure range from atmospheric pressure of approximately 10^3 hPa down to a high vacuum of 3 ×

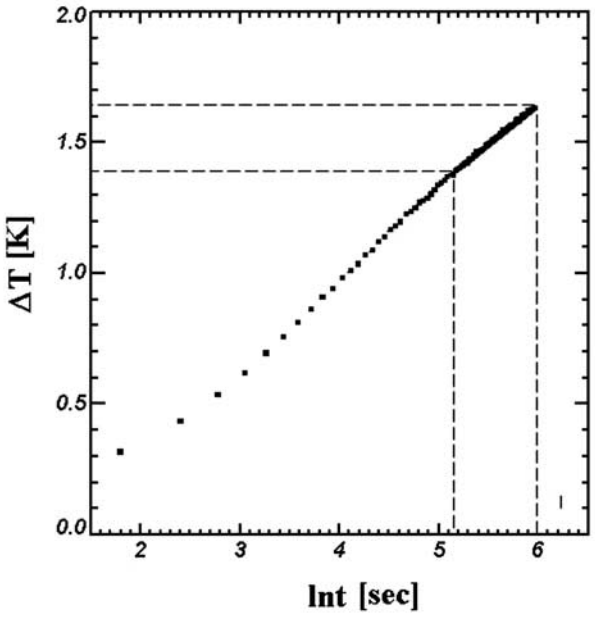

Figure 3. Typical temperature gradient versus natural logarithm of time measurement curve obtained with the TP02 probe for the 1.0–1.25 mm glass beads. The dashed lines indicate the part used for the calculation of the thermal conductivity by linear regression.

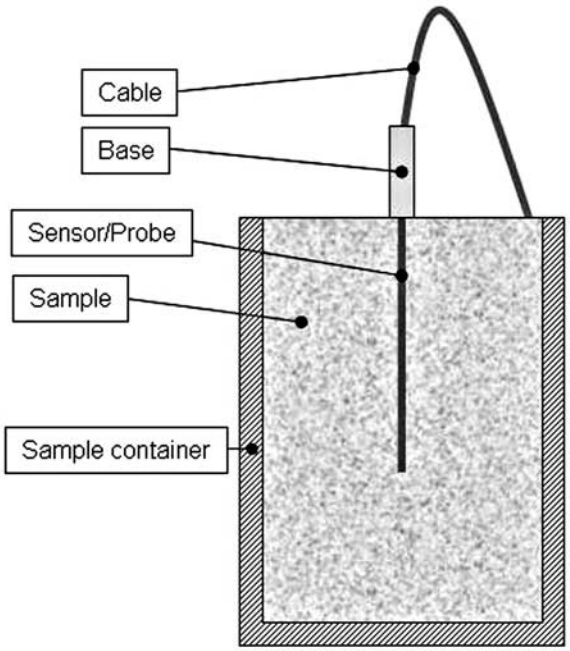

Figure 4. Setup of probe and sample during measurements.

10^{-4} hPa. The measurement setup for this task consisted of the following:

[9] 1. A sample container (dimensions are diameter = 0.265 m, height = 0.34 m) filled with the respective glass spheres. These "large" containers guaranteed that no boundary effects occurred during a measurement (see section 4).

[10] 2. A vacuum chamber with a rotary vane pump to generate a medium vacuum of approximately 10^{-2} hPa and a turbomolecular pump to establish a high vacuum of about 10^{-5} hPa.

[11] 3. A pressure measurement system.

[12] 4. An adjustable supply of nitrogen gas, which allowed to establish different pressure levels.

[13] 5. The TP02 measurement probe described in section 4 with the corresponding data logger. The setup of probe and sample during a measurement is shown in Figure 4.

[14] The measurement procedure was the same for all samples and is outlined in the following:

[15] 1. The sample container was filled with the particular glass spheres and placed in the vacuum chamber. Then the TP02 thermal conductivity probe was mounted in the center of the specimen. After making sure that the probe and the container were fixed in place, the vacuum chamber was closed.

[16] 2. Next, vacuum conditions were established by first using the rotary vane pump and subsequently the turbomolecular pump. This process took up to several hours depending on the grain size of the specimen. Constant pressure was established by means of an adjustable flow of nitrogen gas. The gas flow was corrected manually until an equilibrium between incoming (from the nitrogen gas cylinder) and outgoing gas flux (via the pumps) was reached.

[17] 3. Then a thermal conductivity measurement was performed. At each pressure level three measurements were taken. The thermal conductivity of the glass sphere samples for the corresponding pressure level was determined as the arithmetic mean of these three values. The time interval between the measurements had to be chosen to be long enough that the sample and the probe could reach again a thermal equilibrium state after completion of the heating period. Depending on the particular grain size and pressure level this took quite a long time. The temperature gradient in the sample was logged continuously, not only during measurement. This was used to check if thermal equilibrium was reached. For measurements at pressures of approximately 10^3 hPa the time periods between measurements were about 10 min. Under vacuum it took about a few hours until thermal equilibrium was reached again. The longest waiting periods were those for the smallest glass spheres under high vacuum (only two measurements per day were possible). Correspondingly, the effective thermal conductivity for these samples was the smallest (Table 2).

6. Results

[18] In the following the results obtained from the performed measurements are presented. The thermal conductivity values determined for the single grain sizes at twelve pressure levels are given in Table 2. The listed conductivities are the mean values of the results of three measurements taken at each pressure level. In Figure 5 the dependence of the determined effective thermal conductivity on the particular pressure is illustrated in a semilogarithmic scale for each grain size of the glass spheres. For all grain sizes the well-known s-shaped appearance of the conductivity versus common logarithm of pressure can be observed. This profile results from the change of the gaseous contribution to the effective thermal conductivity as a function of pressure. For pressures higher than 100 hPa the conductivity values reside around 0.17 W m^{-1} K^{-1} for all grain sizes. The measurement results for the glass beads of 0.15 and 0.375 mm mean diameter at lower pressures are consistent with the data obtained by *Presley and Christensen*

Table 2. Mean Effective Thermal Conductivity Values Found at 12 Pressure Levels for Glass Spheres of Five Different Grain Sizes[a]

	Grain Size (mm)				
Pressure (hPa)	0.1–0.2	0.25–0.5	1.0–1.25	2.0–2.3	3.8–4.3
0.0003	0.008	0.008	0.015	0.021	0.039
0.0008	0.008	0.008	0.016	0.021	0.039
0.008	0.008	0.009	0.016	0.021	0.040
0.05	0.008	0.010	0.019	0.026	0.046
0.1	0.009	0.011	0.023	0.031	0.052
0.5	0.013	0.019	0.041	0.056	0.082
1.0	0.017	0.027	0.055	0.073	0.094
5.0	0.041	0.065	0.103	0.116	0.130
10	0.057	0.084	0.124	0.133	0.141
50	0.110	0.129	0.145	0.152	0.155
100	0.135	0.148	0.163	0.159	0.157
500	0.163	0.169	0.169	0.170	0.159

[a]The conductivity values are in W m^{-1} K^{-1}. The different grain sizes are indicated by different colors. The standard deviations mainly ranged between 0.001 and 0.005 W m^{-1} K^{-1}. For the case of the two smallest grain size fractions and pressure levels below 5.0×10^{-1} mbar it was an order of magnitude smaller.

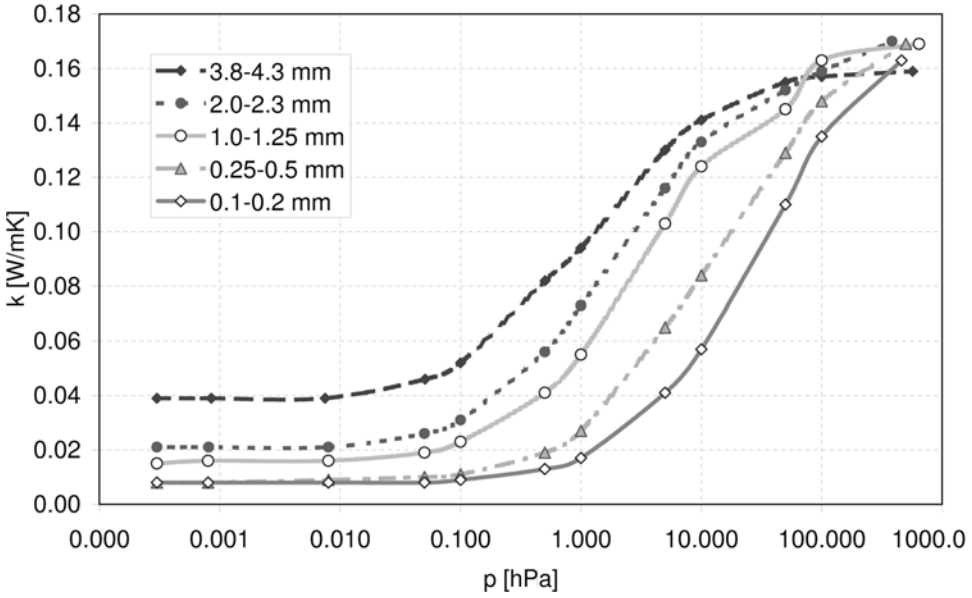

Figure 5. Measured effective thermal conductivity of glass spheres of different grain size as a function of the respective pressure displayed on a semilogarithmic scale.

[1997a] for glass beads of 0.1 and 0.5 mm at 0.6 hPa (0.01 and 0.02 W m^{-1} K^{-1}, respectively). At a higher pressure of approximately 100 hPa, *Presley and Christensen* [1997a] determined a conductivity value of 0.1 W m^{-1} K^{-1} for the 0.1 mm glass beads and a value of 0.17 W m^{-1} K^{-1} for the 0.5 mm glass beads. Our value for the 0.1 mm fraction at this pressure is slightly higher (0.135 W m^{-1} K^{-1}), while the conductivity found for the 0.25–0.5 mm glass beads is smaller (0.148 W m^{-1} K^{-1}). Furthermore, the measured thermal conductivity values are consistent with the experimental results reported by *Reichenauer et al.* [2007], who performed similar measurements on glass spheres with a grain size of 1 mm, and with the conductivity of approximately 0.005 W m^{-1} K^{-1} for 0.15 mm glass beads in high vacuum (0.0004 hPa) determined by *Wechsler and Glaser* [1965].

6.1. Pore Sizes

[19] In the region between approximately 0.1 and 100.0 hPa where a strong decrease of the thermal conductivity occurs, equation (8) is valid. At the beginning and end of this region the largest deviations from the linear relation appear. Below a pressure of approximately 0.01 hPa no significant change of the effective thermal conductivity is observed. This indicates that below the given pressure limit the influence of the gas phase on the thermal conductivity is not significant. Therefore, the effective conductivity in this pressure domain is determined by conduction via the solid phase and

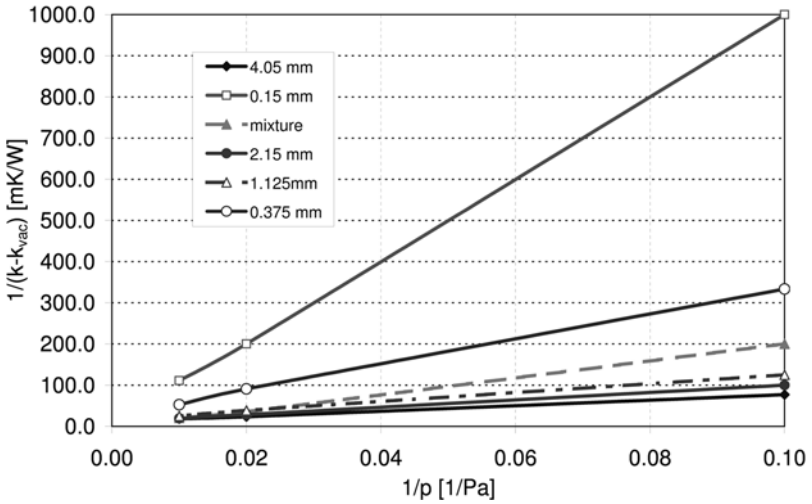

Figure 6. Reciprocal thermal conductivity change versus reciprocal pressure plotted for the different grain size fractions.

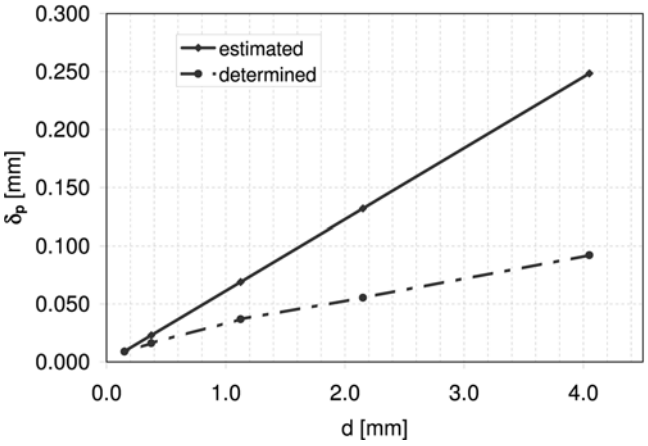

Figure 7. Pore sizes determined from the measurement data using relation (9) (chain-dotted line), and pore sizes estimated by equation (3) (solid line); these sizes are plotted against the mean grain size.

radiation. This meets relation (8) for the vacuum conductivity. From the given measurement data the pore sizes of the different samples were determined using relation (9). The obtained reciprocal conductivity change versus reciprocal pressure is shown in Figure 6. In each case the conductivity value measured at the lowest pressure level of 0.0003 hPa was used for the vacuum conductivity k_{vac}. The derived d/δ_p ratios were 44 for the biggest glass beads with a mean diameter of 4.05 mm, 38.8 for the 2.15 mm glass beads, 30.6 for the 1.125 mm glass beads, 23.3 for the 0.375 mm glass beads, and 17.1 for the 0.15 mm glass beads fraction. *Woodside and Messmer* [1961] calculated a d/δ_p value of 72.6 for their glass bead sample with a mean diameter of 0.358 mm. For a lead shot sample of 1.23 mm grain size they computed a ratio of 170. The d/δ_p ratios of the comparable size fractions of the glass beads, namely the 0.375 mm and 0.358 mm grains, differ by about a factor of 3. The higher ratio of *Woodside and Messmer* [1961] is maybe due to the fact that the used conductivity value was too high, since the lowest pressure level they investigated was above 0.013 hPa. A second possible explanation, mentioned by *Presley and Christensen* [1997a], is that Woodside acknowledged that the conductivity measurement probe used by *Woodside and Messmer* [1961] sometimes produced higher values. Furthermore, the pore sizes were also determined using equation (3). Except for the smallest glass beads, these strongly differ from the values derived from the measurement data. For the smallest grain size fraction the pore size derived from the measurements and the pore size determined from equation (3) are in the same range. In Figure 7 the pore sizes determined from the data and estimated by equation (3) are shown as a function of grain size.

6.2. Knudsen Number

[20] The behavior of the gas in the pores under different pressure conditions can be described by the Knudsen number (see section 2). Therefore, this dimensionless factor was estimated for these measurements. In Figure 8 the derived Knudsen number as a function of pressure is displayed for various conditions in a double logarithmic scale. The boundary of Kn = 10, where the gaseous conductivity becomes negligible, is indicated as a thick black line. First, the pore sizes calculated from equation (3) were used to estimate the Knudsen number for the given experimental environment. The results for the biggest and for the smallest grain size fraction are shown, since the results for the other grain size fractions lie in between these two. The before stated pressure limit of 0.01 hPa clearly satisfies Kn>10. Below this pressure the gaseous conductivity becomes negligible. Additionally, the Knudsen numbers were calculated for Martian conditions (gas is CO_2, d_g = 0.46 nm, T = 240 K). This causes a shift of the Knudsen number versus pressure curve by 0.0015 hPa toward lower pressures. Second, the Knudsen number was also evaluated for the pore sizes determined from the data (see subsection

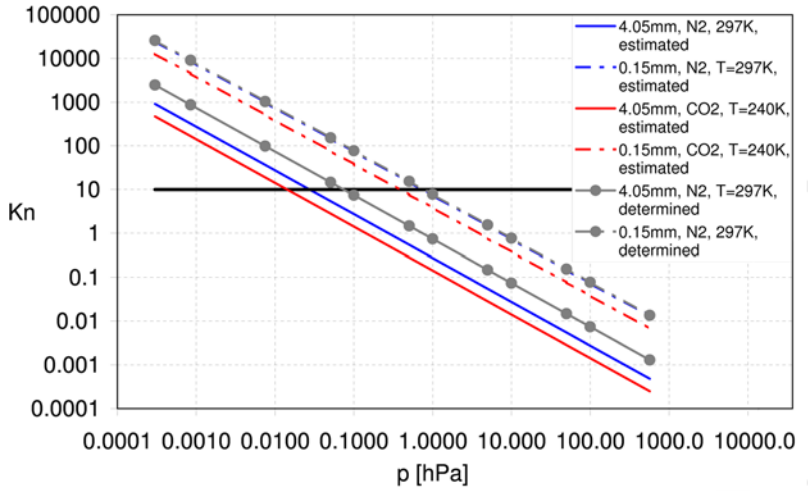

Figure 8. Derived Knudsen number versus pressure for different conditions of grain size, temperature, and interstitial gas displayed on a double logarithmic scale.

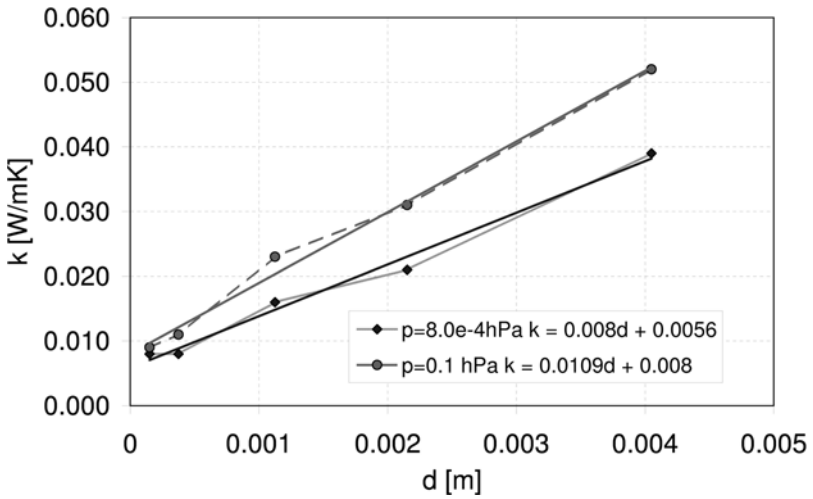

Figure 9. Thermal conductivity as function of the grain size for two low pressure levels. Both show a linear behavior.

6.1). These pore sizes are significantly smaller than the estimated ones in the case of the biggest glass spheres, but the values get closer with decreasing grain size. The largest pore size difference occurs for the 4.05 mm glass beads. This causes a shift of the pressure limit for the largest grain size fraction toward higher pressures, while hardly any shift occurs for the 0.15 mm glass bead fraction. Furthermore, it is noticeable that Knudsen flow is established at significantly higher pressures for the smallest glass spheres than for the biggest glass spheres.

6.3. Vacuum Conductivity

[21] Below a pressure of about 0.01 hPa the contribution of the gaseous phase becomes negligible. In this region equation (8) is valid. A grain size–dependent splitting up of the vacuum conductivity can be observed. The highest values at hand are those for the biggest glass beads. Moreover, nearly identical thermal conductivity values were found for the two smallest fractions of glass spheres (the 0.15 and 0.375 mm fraction) in the pressure range below 0.01 hPa. In Figure 9 the variation of the conductivity as a function of grain size is plotted for two low pressure levels, namely, 0.0008 and 0.01 hPa. Here the observed decrease of conductivity with decreasing particle size is linear. This is in agreement with model calculations performed by *Tavman* [1996], who also found a decrease of the effective thermal conductivity with decreasing grain size. The linear relation between grain size and effective thermal conductivity for the determined set of conductivity data is valid for pressures below approximately 0.05 hPa. Above this pressure conductivity versus grain size is linear in the double logarithmic scale. This is in agreement with the results of *Presley and Christensen* [1997a, 1997b]. In Table 3 the parameters slope s, axis intercept a, and goodness of fit R^2, which were determined by linear regression from the conductivity versus grain size data, are given for the five pressure levels from 0.1 down to 0.0003 hPa. The vacuum conductivity is composed of the conduction contributions from the solid phase and of the radiative contribution. For the radiative part, relation (5), which was proposed by *Schotte* [1960], was evaluated. The derived radiative conductivity as a function a of temperature for different particle sizes is given in Figure 10. It can be observed that the larger the particles are, the higher is the radiative contribution. Furthermore, for larger particles a stronger temperature dependence can also be noted. The radiative contribution calculated for the biggest glass spheres (0.0044 W m^{-1} K^{-1}) is approximately 1 order of magnitude smaller than the effective thermal conductivity for this size fraction under vacuum (0.04 W m^{-1} K^{-1}). In the case of the smallest glass beads of 0.15 mm the radiative contribution (0.0002 W m^{-1} K^{-1}) is two magnitudes smaller than the measured vacuum conductivity (0.008 W m^{-1} K^{-1}).

6.4. Effective Thermal Conductivity of a Mixture of Glass Spheres

[22] Additionally, the thermal conductivity of a mixture of glass spheres was investigated at different pressure levels. The mixture was composed of glass spheres with the size ranges 3.80–4.30 mm, 2.00–2.30 mm, and 1.00–1.25 mm. From each grain size equal volume fractions were added (see section 3). The thermal conductivity values determined for the mixture are listed in Table 4. A plot of the effective thermal conductivity as a function of pressure is shown in Figure 11 in a semilogarithmic scale. For comparison the data are plotted along with the values determined for the single grain sizes. It is striking that the thermal conductivity of the mixture shows a stronger rise with pressure than the conductivity determined for the

Table 3. Slope, Axis Intercept, and Goodness of Fit Determined for the Thermal Conductivity Versus Grain Size Relation[a]

Pressure (hPa)	s(W m^{-2} K^{-1})	a(W m^{-1} K^{-1})	R^2
0.0003	0.008	0.0056	0.9906
0.0008	0.008	0.0059	0.9882
0.008	0.0079	0.0063	0.9895
0.05	0.0096	0.0067	0.9954
0.1	0.0109	0.008	0.9924

[a]The values are given for the five lowest pressure levels. For those the linear relation fits best.

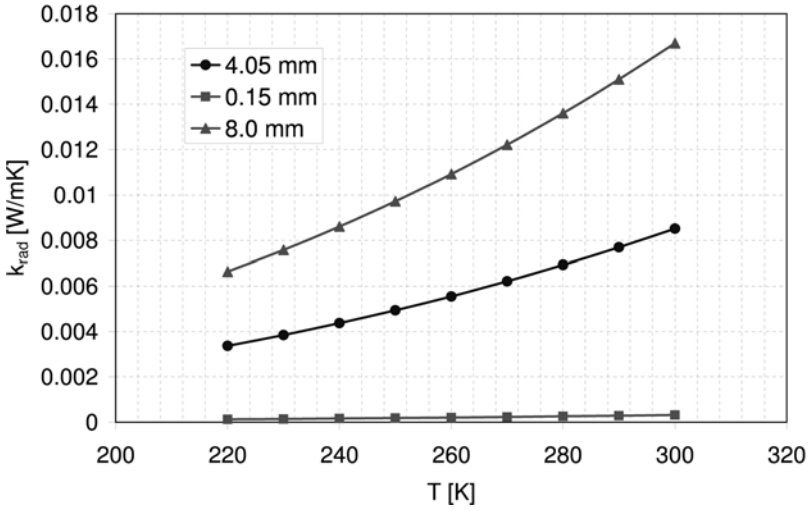

Figure 10. Radiative conductivity calculated by relation (5) as a function of temperature. Three different particle sizes are displayed.

single grain sizes. At 500 hPa the thermal conductivity of the mixture is significantly higher than the conductivities found for the single grain sizes at this pressure level. Furthermore, it can be seen clearly that below 0.1 hPa the conductivity values of the mixture match the values found for the 0.375 and 0.15 mm glass bead fractions. In summary, the behavior of the glass sphere mixture significantly deviates from the behavior of the single grain size samples. A possible explanation for this different behavior may be the different texture of the mixture, since the voids between the bigger glass spheres can be filled by the smaller ones, which leads to smaller pores. This point is also indicated by the porosity of 0.355 determined for the mixture. This interpretation would explain the matching conductivities at low pressures, where the mixture acts like a granular material with a grain size smaller than the grain sizes of which the mixture is composed of, while at high pressures an increase of the thermal conductivity over that of the single grain sizes occurs owing to increased conduction via the solid phase. A similar behavior in the case of a grain size mixture was found by *Woodside and Messmer* [1961]. Natural samples investigated by *Presley and Craddock* [2006] did not display such an enhancement of the thermal conductivity of a mixture of grain sizes at high pressure, compared to the thermal conductivity of the single grain sizes at high pressure. The conductivity data obtained for the mixture were also analyzed using relation (9). A representative pore size of 0.0262 mm was found, which is somewhat smaller than the pore size found for the smallest glass bead fraction of the mixture. The evaluation performed on the single grain sizes was used to produce the diagram shown in Figure 12. Here the d/δ_p ratios are plotted first as a function of pore size and second as a function of grain size. A polynomial fit was performed on each of the functions. From this graph, pore size and grain size, respectively, can be determined in a direct way. This was used to determine the d/δ_p ratio for the pore size derived from the data obtained for the mixture. A d/δ_p value of 27.1 was found. The corresponding particle diameter is 0.806 mm, which is equal to the weighted arithmetic mean of the mean grain sizes used for the mixture (each grain size is weighted with 0.33, since the mixture is composed of equal volumes of three grain sizes). This result is quite reasonable, although it is different from the analysis of a mixture performed by *Woodside and Messmer* [1961], who proposed that the effective diameter is given as the harmonic mean of the particle diameters of the mixture components. The derived effective diameter was used to calculate the mean mixture pore size by equation (3). A pore size value of 0.036 mm was determined.

7. Summary and Conclusions

[23] The effective thermal conductivity of glass spheres of different grain sizes was investigated under varying pressure conditions. The determined values are in good agreement with data obtained from previous studies. In addition, a well defined mixture of different grain sizes was examined. This specimen showed a different behavior compared to the tests with single grain sizes. The results indicate that at lower pressures the mixture can be described as an effective granular material with a grain size smaller

Table 4. Effective Thermal Conductivity Values Found for the Mixture of Different Grain Sizes[a]

Pressure (hPa)	k (W m^{-1}K^{-1})
0.0003	0.009
0.0008	0.009
0.008	0.009
0.05	0.011
0.1	0.014
0.5	0.037
1.0	0.058
5.0	0.124
10	0.144
50	0.186
100	0.198
500	0.219

[a]The standard deviation for these values is in the same range as for the conductivity values obtained for the single sizes.

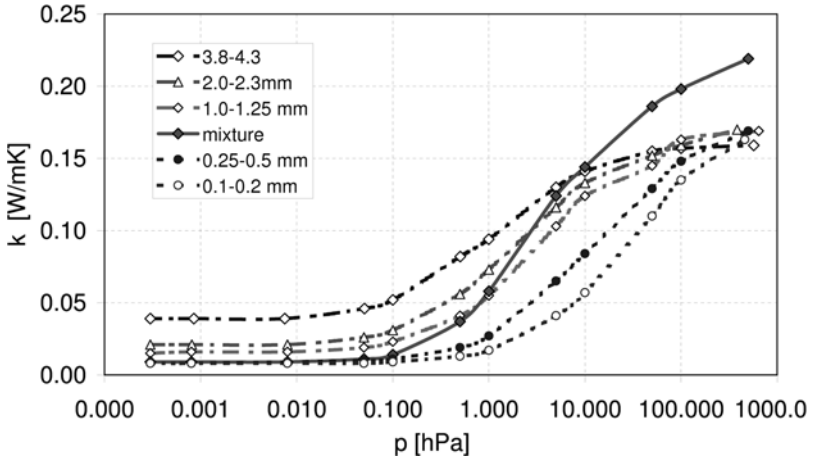

Figure 11. Thermal conductivity values determined for an equivolume mixture of glass spheres of three size fractions compared to the conductivity values determined for all the single-sized samples. The data are given on a semilogarithmic scale. The mixture components are indicated by chain-dotted lines, while the two smallest grain size fractions are indicated by dashed lines.

than those of which the mixture is composed of. This case is most important, since granular material on planetary surfaces is always a compound of several different grain sizes. The pore sizes of the different samples were determined using the concept proposed by *Woodside and Messmer* [1961] and relation (3) given by *Kaviany* [1998]. For the single-sized samples pore sizes about two magnitudes smaller than the grain sizes were determined from the measurement data. For the mixture a pore size valid for the weighted mean of the grain size fractions used for the mixture was derived. The pore sizes calculated from equation (3) are systematically larger, the larger the considered particle size. For the small size fraction the determined and estimated pore size are in the same range. The Knudsen number, a factor describing the gas behavior in the pores of a granular material, was evaluated for the measurement conditions and also for Martian conditions. The results show that the behavior under Martian conditions differs only slightly from the laboratory conditions. From the measurements and the Knudsen number can be seen that the pressure region representing Martian conditions around 6 hPa is quite sensitive to variations in grain size. For very small grain sizes Knudsen diffusion might be reached, for larger ones not. This implies a significant thermal conductivity difference depending on the grain size and a high sensitivity to pressure changes. Furthermore, a significant grain size dependence was found for the radiative contribution given by *Schotte* [1960]. The larger the particles are, the higher are the radiative conductivity and the temperature dependence. Another fact is that the thermal conductivities found for the 1.125, 2.15, and 4.05 mm glass spheres are in the same range as the conductivities determined for the lunar regolith during the Apollo missions. The studies performed in this work complement and extend previous measurements.

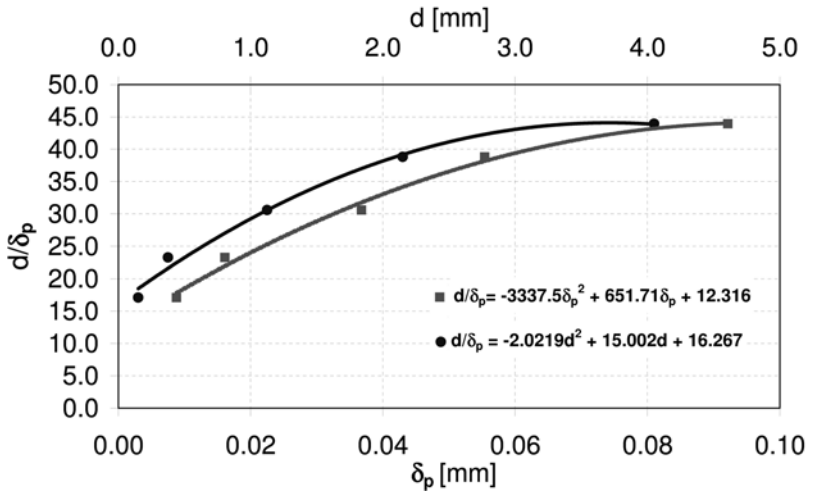

Figure 12. Grain size to pore size ratio d/δ_p as a function of pore and grain size.

Notation

α_{sample} thermal diffusivity of the sample.
δ_p mean pore size diameter.
ϵ emissivity.
λ mean free path of gas molecule.
ψ porosity.
σ Stafan-Boltzmann constant, $\sigma = 5.67 \times 10^{-8}$, W m^{-1} K^{-1}.
ρ_{bulk} density of granular material.
ρ_{solid} density of particle solid material.
a axis intercept.
B factor, $B = \frac{k_B T}{\sqrt{2}\pi d_g^2}$.
d_g diameter of gas molecule.
d_p diameter of particles.
k_b Boltzmann constant, 1.38110^{-23} J K^{-1}.
k_{eff} effective thermal conductivity.
k_g conductivity of gas.
k_g^0 conductivity of gas at standard pressure of 1013 hPa.
k_{rad} conductivity due to radiation.
k_s conductivity of solid material.
k_{vac} effective conductivity under vacuum conditions.
Kn Knudsen number, ratio mean free path of gas molecule to characteristic pore length.
p pressure, hPa.
P_{heat} heating power, W m^{-1} K^{-1}.
R^2 goodness of fit.
R_{sample} radius of sample.
r_{sensor} radius of sensor.
s slope.
T temperature.
t time.
$t_{\max}$ point in time after the onset of heating after which boundary effects occur.
t_{trans} time period of nonlinear temperature versus ln(t) development.
V_f volume occupied by fluid (e.g., gas).
V_{tot} volume of the sample.
W slope of the linear relation between effective thermal conductivity and gas conductivity.

[24] **Acknowledgments.** This work was supported by the project "Development of Thermal Sensors for Planetary Surface Layers" (project L317-N14) of the Translational Research Program of the Austrian Science Fund (FWF).

References

Carslaw, H. S., and J. C. Jaeger (1959), *Conduction of Heat in Solids*, 2nd ed., Clarendon Press, Oxford, U. K.

Chauk, S. S., and L.-S. Fan (1998), Heat transfer in packed and fluidized beds, *Handbook of Heat Transfer*, 3rd ed., chap. 13, McGraw-Hill, New York.

Goodhew, S., and R. Griffiths (2004), Analysis of thermal-probe measurements using an iterative method to give sample conductivity and diffusivity data, *Appl. Energy*, *77*, 205–223.

Howell, J. R., and M. P. Mengüc (1998), Radiation, *Handbook of Heat Transfer*, 3rd ed., chap. 7, McGraw-Hill, New York.

Huetter, E. S., and N. I. Koemle (2008), Determination of the radiative contribution to the thermal conductivity to the effective thermal conductivity of a granular medium under vacuum conditions, paper RAD_8 presented at 5th European Thermal Sciences Conference, Eindhoven Univ. of Technol., Eindhoven, Netherlands, 18–22 May.

Kaviany, M. (1994), *Principles of Heat Transfer in Porous Media*, 2nd ed., Springer, New York.

Kaviany, M. (1998), Heat transfer in porous media, *Handbook of Heat Transfer*, 3rd ed., chap. 9, McGraw-Hill, New York.

Koemle, N. I., et al. (2007), Thermal conductivity measurements of road construction materials in frozen and unfrozen state, *Acta Geotech.*, *2*, 127–138.

Merrill, R. B. (1969), Thermal conduction through an evacuated idealized powder over the temperature range of 100° to 500°K, *Nasa Tech. Note*, D-5063, 82 pp.

Presley, M. A., and P. R. Christensen (1997a), Thermal conductivity and measurements of particulate materials: 2. Results, *J. Geophys. Res.*, *102*, 6551–6566.

Presley, M. A., and P. R. Christensen (1997b), The effect of bulk density and particle size sorting on the thermal conductivity of particulate materials under Martian atmospheric pressure, *J. Geophys. Res.*, *102*, 9221–9229.

Presley, M. A., and R. A. Craddock (2006), Thermal conductivity measurements of particulate materials: 3. Natural samples and mixtures of particle sizes, *J. Geophys. Res.*, *111*, E09013, doi:10.1029/2006JE002706.

Reichenauer, U., U. Heinemann, and H. P. Ebert (2007), Relationship between pore size and the gas pressure dependence of the gaseous thermal conductivity, *Colloids Surf. A*, *300*, 204–210.

Schotte, W. (1960), Thermal conductivity of packed beds, *AIChE J.*, *6*, 63–67.

Starukhina, L. V. (2000), Characterisitics of the contact between regolith particles: Their influence on the physical properties of regoliths, *Sol. Syst. Res.*, *34*, 295–302.

Tavman, I. H. (1996), Effective thermal conductivity of granular porous materials, *Int. Comm. Heat Mass Transfer*, *23*, 169–176.

Vaniman, D., R. Reedy, G. Heiken, G. Olhoeft, and W. Mendell (1991), *Lunar Sourcebook: A User's Guide to the Moon*, Cambridge Univ. Press, Cambridge, U. K.

Vos, B. H. (1955), Measurements of thermal conductivity by a non-steady-state method, *Appl. Sci. Res.*, 125–438.

Watson, K. (1964), The thermal conductivity measurements of selected silicate powders in vacuum from 150° to 350°K, Ph.D. thesis, Calif. Inst. of Technol., Pasadena.

Wechsler, A. E., and P. E. Glaser (1965), Thermal properties of postulated lunar surface materials, *Icarus*, *4*, 335–352.

Wechsler, A. (1992), *Compendium of Thermophysical Property Measurement Methods*, vol. 2, Plenum Press, New York.

Woodside, W., and J. H. Messmer (1961), Thermal conductivity of porous media: I. Unconsolodated sands, *J. Appl. Phys.*, *32*, 1688–1699.

E. S. Huetter, G. Kargl, E. Kaufmann, and N. I. Koemle, Space Research Institute, Austrian Academy of Sciences, Schmiedlstrasse 6, A-8042 Graz, Austria. (erika.huetter@oeaw.ac.at)